INTERNATIONAL JOURNAL OF CLIMATOLOGY
Int. J. Climatol. **32**: 2007–2019 (2012)
Published online 5 August 2011 in Wiley Online Library
(wileyonlinelibrary.com) DOI: 10.1002/joc.2414

RMetS
Royal Meteorological Society

Developing site-specific future temperature scenarios for Northern Ireland: addressing key issues employing a statistical downscaling approach

Donal Mullan,[a]* Rowan Fealy[b] and Dave Favis-Mortlock[c]

[a] *School of Geography, Archaeology and Palaeoecology, Queen's University Belfast, Belfast BT71NN, Northern Ireland, UK*
[b] *Department of Geography, National University of Ireland, Maynooth, Republic of Ireland*
[c] *Environmental Change Institute, University of Oxford, South Parks Road, Oxford OX1 3QY, England, UK*

ABSTRACT: Modelling future temperature changes is a crucial step in the climate change impacts analysis stage for a wide range of environmental and socioeconomic sectors. A scale mismatch exists, however, between the coarse spatial resolution at which general circulation models (GCMs) project future climate change scenarios, and the finer spatial resolution at which impact modellers require such projections. Various downscaling techniques can be used to bridge this gap, with statistical downscaling methods emerging as a popular, low-cost and accessible means of developing site-specific future scenarios. Despite its widespread use, little attention has been paid to some of the key issues in statistical downscaling which are central to the development of the future scenarios, including GCM grid-box choice and the effects of modifying the calibration period. In this study, such issues are examined with respect to the development of site-specific future temperature scenarios for nine climatological stations across Northern Ireland. Results indicate that the more remote grid box of the two analysed is most strongly correlated with maximum and minimum temperatures, illustrating the importance of examining potential spatial offsets in the predictor-predictand relationship. In addition, modifications to the calibration period result in only minor differences to seasonal calibration and validation values as well as resultant future projections, indicating that longer calibration periods do not always offer improvements over shorter periods. Future downscaled scenarios reveal considerable warming across all sites and seasons, with large inter-GCM differences apparent. This underlines the importance of employing multiple GCMs and emissions scenarios to help address the uncertainties inherent in global climate modelling. This study illustrates the potential of statistical downscaling methods in generating high-resolution future climate change scenarios appropriate to the requirements of impact modellers, provided a thorough analysis of some of the key issues that shape the character of the future scenarios are fully explored. Copyright © 2011 Royal Meteorological Society

KEY WORDS climate change; statistical downscaling; Northern Ireland; temperature; calibration period; grid box; predictor selection; spatial offsets

Received 10 September 2010; Revised 29 June 2011; Accepted 1 July 2011

1. Introduction

Information concerning future changes in temperature and its variability is necessary to model various surface processes at global and local scales across a range of disciplines in both the natural and social sciences (Anandhi *et al*., 2009). Temperature influences human health, particularly through extremes leading to hypothermia or heat stress (Ballester *et al*., 2003). Temperature also influences a range of other natural systems including botany, through phenological events such as the timing of flowering and breeding (Carroll *et al*., 2009); and agriculture, from crop and livestock disease (Thornton *et al*., 2009) to the growth and yield of crops (Wiik and Ewaldz, 2009). In addition to the wide-ranging impacts on natural systems, temperature influences socioeconomic systems including transport, particularly through high extremes leading to stresses on railway tracks (Chapman *et al*., 2008) and low extremes exerting strain on road salt supplies (Handa *et al*., 2006). Other impacted socioeconomic systems include the built environment, where thermal fatigue leads to the disintegration of building stone (Gómez-Heras *et al*., 2006); energy consumption, where lower temperatures generally increase demand (Lam *et al*., 2004); and tourism, where prolonged periods of sunshine and associated high temperatures frequently lead to increased levels of holidaying and recreation (Gómez-Martín, 2005). Given the sensitivity of such a vast range of impact sectors to temperature, the need for climate impact assessments that examine future temperature changes is of significant importance in order to

* Correspondence to: Donal Mullan, School of Geography, Archaeology and Palaeoecology, Queen's University Belfast, Belfast BT71NN, Northern Ireland, UK. E-mail: dmullan15@qub.ac.uk

develop adaptation strategies to cope with such changes. In addition, as most climate impact models operate on a fine spatial scale, future climate change projections must be provided at the same spatial resolution to be suitable as input to impact models (Wilby and Dawson, 2007). The most credible tools for projecting future climate change (general circulation models (GCMs)) can only calculate atmospheric processes at a horizontal spatial resolution of several hundred kilometres, however, which is too coarse to be useful as input data for impact models (Schubert and Henderson-Sellers, 1997).

1.1. Methods for generating finer spatial resolution

Downscaling techniques are utilized to bridge this gap between what GCMs can provide and what impact assessors require. Downscaling can broadly be grouped into two main types; dynamical or statistical downscaling (Wilby and Dawson, 2007). Dynamical downscaling refers to the nesting of a high-resolution Regional Climate Model (RCM) within a coarser resolution GCM. Several studies (e.g. Murphy, 1999; Bergström *et al.*, 2001; Hulme *et al.*, 2002; Arnell *et al.*, 2003) have illustrated the success of dynamical downscaling approaches. The main advantage of dynamical downscaling is that RCMs, being physically based, can resolve small-scale atmospheric features such as low-level jets, or orographic precipitation, better than the host GCM (Wilby and Dawson, 2007). Statistical downscaling methods, meanwhile, rely on identifying and developing mathematical transfer functions or empirical relationships between observed large-scale predictors and the surface environmental variable of interest (local-scale predictands) (Wilby and Dawson, 2007). One common statistical downscaling approach is perfect-prognosis downscaling (e.g. Wilks, 2006; Maraun *et al.*, 2010). This approach is based on the concept that regional climate is governed by the relationship between the synoptic climate state and local physiographic features, represented by a statistical model, with GCM output then fed into the statistical model for estimation of corresponding local and regional climate variables (Wilby *et al.*, 2004). The predictor–predictand relationship should explain a large amount of the observed variability and the expected changes in the mean climate should lie within the range of its natural variability (von Storch *et al.*, 1993). Statistical downscaling has become a popular method of creating downscaled climate scenarios. Some statistical downscaling techniques facilitate the creation of ensemble forecasts, which provide uncertainty analysis of future projections (Wilby and Dawson, 2007). Their ability to provide site-specific information is fundamental to climate change impact studies and is often the only practicable means of generating climate scenarios for point-scale processes such as soil erosion (e.g. Favis-Mortlock and Boardman, 1995). Wilby *et al.* (2004) indicate that one of the primary advantages of statistical downscaling techniques is that they are computationally inexpensive and thus can be easily applied to output from different GCM experiments.

1.2. Downscaling temperature in Ireland

Contrasting downscaling techniques have been used to develop future temperature projections at a finer spatial resolution in Ireland. Statistical downscaling methods were used in the development of future temperature scenarios for 14 sites across the Republic of Ireland (Fealy and Sweeney, 2008). Results from this study revealed mean temperature increases of 2.0–2.7 °C for the 2080s, with autumn projected to warm most, inland locations projected to warm at a higher magnitude than coastal locations, and extremes projected to include increased hot-day temperatures and a decreased incidence of frost days. The highest resolution temperature scenarios published for Northern Ireland, meanwhile, were developed using an RCM nested within the UK Hadley Centre GCM in a climate change scoping report by the Scotland and Northern Ireland Forum For Environmental Research (SNIFFER) (Arkell *et al.*, 2007), providing future temperature scenarios at a spatial resolution of 50 km. Findings indicated a 1–3.5 °C warming by the 2080s, with autumn and summer projected to warm most, extremely warm days projected to become more frequent and hotter, and the number of cold days projected to decline.

Statistical downscaling methods are employed in this study to examine, for the first time, future changes in temperature across Northern Ireland at a site-specific spatial resolution. A popular decision-support tool for assessing local climate change impacts, the Statistical DownScaling Model (SDSM) (Wilby and Dawson, 2007), is the specific tool used to develop these scenarios. SDSM version 4.2 (Wilby and Dawson, 2007) is a Windows™-based decision support tool for assessing local climate change impacts using a robust statistical downscaling technique. SDSM facilitates the rapid development of multiple, low-cost, single-site scenarios of daily surface weather variables under current and regional future climate forcing (Wilby and Dawson, 2001; Wilby *et al.*, 2002). SDSM is frequently described as a hybrid between a regression-based approach and a weather generator, because large-scale daily circulation patterns and atmospheric moisture variables are used to condition local-scale weather generator parameters at individual sites (Wilby and Harris, 2006). The underlying philosophy of SDSM relies on the establishment of multiple regressions between local-scale predictands (such as daily rainfall and temperature) and large-scale predictors (such as mean sea level pressure and surface vorticity (Wilby and Dawson, 2007). The established relationships are then applied to the circulation simulated by a GCM in order to generate projections of local climate, motivated by the assumption that GCMs simulate large-scale atmospheric circulation better than they simulate surface climate variables (Murphy, 2000).

In this study, output from three GCMs and two emissions scenarios are used to downscale daily maximum and minimum temperatures to the point-scale at nine climatological stations across Northern Ireland. Use of multiple GCMs and emissions scenarios helps address uncertainties inherent in global climate modelling and

makes possible the generation of a range of equally plausible site-specific future scenarios. For three future time slices, results are presented as temperature changes from the 1961–1990 modelled baseline period. In addition, results are provided on a seasonal and spatial basis in order to examine differences in the magnitude of warming across different sites and at different times of the year. Finally, future changes in temperature extremes are presented, since extremes are frequently the variables of most interest to impact modellers.

2. Key issues in the downscaling process

An additional aim of this study is to examine some of the issues and choices associated with statistical downscaling that shape the nature of the future downscaling results.

2.1. Non-stationarity

The issue of non-stationarity, in particular, may seriously undermine the realism of future scenarios (Wilby, 1997). Non-stationary predictor–predictand relationships may arise from: (1) An incomplete set of predictor variables that excludes low-frequency climate behaviour; (2) An inadequate sampling or calibration period for the chosen predictor–predictand relationships; or (3) Situations in which the climate system changes through time (Wilby, 1998). Case (1) is less significant for downscaling temperature than precipitation, since a much higher proportion of the explained variance in temperature can be captured given its greater spatial uniformity. Most serious of the three symptoms of non-stationarity is case (3). This is considered the major theoretical weakness of perfect-prognosis statistical downscaling techniques, as their basic assumption is not verifiable, i.e. that statistical relationships derived for the present day climate also hold under future climate forcing (Wilby *et al*., 2004). Predictor–predictand relationships are thus assumed to be time-invariant, yet it is well recognized that transfer functions may become invalid or weights attached to different predictors may change under the future climate regime (Wilby *et al*., 2004). Relationships, therefore, must be critically and carefully assessed as it is impossible to check future climate conditions with observational records (Arnell *et al*., 2003). Tests of stationarity of statistical transfer functions using comparable relationships in RCMs, however, suggest the time-invariance assumption may be robust provided that the choice of predictors is judicious (Charles *et al*., 1999). Empirical methods are not well positioned to resolve case (3), whereas examination of case (2) is possible based upon modifying the calibration period. Downscaling models for temperature calibrated on colder-than-average periods in the observed station data are likely to seriously underestimate future temperatures, whilst models calibrated on warmer periods within the observed record are likely to result in overestimations (e.g. Wilby, 1998). Examination of the length and specific timeframe of the calibration period is therefore conducted in this study and discussed with respect to model calibration, validation, and the resultant impact on future temperatures.

2.2. Predictor selection

Selection of appropriate predictor variables is another key issue in the statistical downscaling process, representing the most critical stage in the shaping of future scenarios. (Wilby *et al*., 2004). According to Wilby *et al*. (2002), predictor variables should be: (1) Physically and conceptually sensible with respect to the predictand; (2) Strongly and consistently correlated with the predictand; (3) Readily available from archives of observed data and GCM output; and (4) Accurately modelled by GCMs. In this respect, and since predictor selection is central to statistical downscaling and the resultant character of the downscaled scenarios, this study affords particular attention to the search for appropriate predictor variables to downscale maximum and minimum temperatures.

2.3. Grid-box choice

A final important consideration in the present study concerns the issue of grid-box choice, given that predictors from the grid box overlying the target station do not always exhibit the strongest correlations with the predictand, as possible spatial offsets in the correlation patterns may exist (Wilby and Wigley, 2000). Brinkmann (2002) echoed this, noting that choice of grid box is critical for capturing the circulation features of significance to the local climate. In previous climate change scoping studies for Northern Ireland, the grid-box choice has emerged as a key problem with respect to developing future scenarios for the region. For example, the SNIFFER report (Arkell *et al*., 2007) on implications of climate change for Northern Ireland identified that the region effectively existed as ocean in the HadCM2 GCM used, thereby presenting a problem of model output appropriateness within this box for application to future climate change scenarios for the region (Betts, 2002). Wilby and Dawson (2001) also addressed the grid-box issue with respect to the UKSDSM data archive (Figure 1), noting that because three of the nine grid cells in the archive are ocean, more realistic estimates of forcing over land areas that are represented by ocean grid boxes could be developed by averaging the two nearest land cells. In the UKSDSM data archive, this involved averaging the Ireland (IR) and Scottish Borders (SB) grid boxes to form a notional NIR grid box. However, as the IR grid-box parameters are derived from the entire island of Ireland, this grid box in isolation (ie. without averaging with other grid boxes) clearly also offers a climatologically sound possibility for downscaling over Northern Ireland. In this respect, both the IR and NIR grid boxes are examined for correlations between maximum and minimum temperatures and a selection of predictors from the UKSDSM data archive (Wilby and Dawson, 2007) for each site and season. The overall aim of the study, therefore, is to develop site-specific future temperature scenarios for Northern Ireland in a manner that

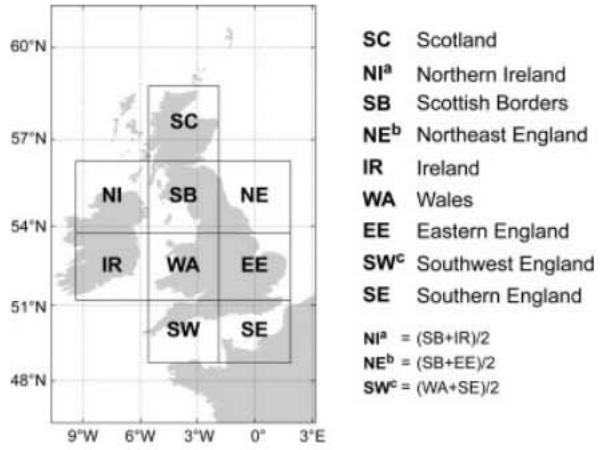

Figure 1. Location and nomenclature of the nine grid boxes used in the UKSDSM data archive (after Wilby and Dawson, 2007).

examines rigorously the core issues of statistical downscaling that shape the character of the future scenarios.

3. Data and methods

3.1. Data sources

3.1.1. Predictands

Observed daily data for maximum and minimum temperatures were obtained for nine climatological stations in Northern Ireland from the Met Office Land Surface Stations Observations data set via the British Atmospheric Data Centre (BADC). The stations were selected on the basis of two main criteria: (1) Completeness of the temperature records to ensure a minimum baseline climatology with thirty years of data from the year 1961; and (2) A wide geographical spread of stations to capture a mixture of coastal and interior locations (Figure 2). An additional site-selection factor, unrelated to this study, was to ensure close proximity of the stations to sites for soil erosion modelling, which forms the basis of an ongoing research project. Temperature data for the period of 1961–1990 exists for all 9 selected stations, but only three of these contain data beyond this (from 1961 to 2000). Thus for model calibration, the period of 1961–1990 was chosen for consistency between sites. However, the three stations with data extending over an extra decade offered an opportunity to extend the calibration period and examine its impact on future downscaled scenarios (this approach is detailed in the Methods section).

3.1.2. Predictors

A total of 29 large-scale surface and atmospheric predictor variables were obtained from the United Kingdom Statistical DownScaling Model (UKSDSM) data archive (Wilby and Dawson, 2007). Variables included both National Centre for Environmental Prediction (NCEP) Reanalysis data (representing 1961–2000 'present-day' large-scale variables) and data from three GCMs (Table I), forced by the A2 and B2 emissions scenarios (Nakicenovic *et al.*, 2000) (representing 1961–2099 future large-scale variables). The NCEP Reanalysis project involved the recovery of land surface, ship, radiosonde, aircraft, satellite and other data to assimilate a quality controlled observed record of large-scale circulation variables and surface climate data spanning the period 1961–2000 (Kalnay *et al.*, 1996). In the UKSDSM data archive, the NCEP data was regridded to a 2:5 3:75° coordinate system, corresponding to the grid coordinates of one of the GCMs used in this study

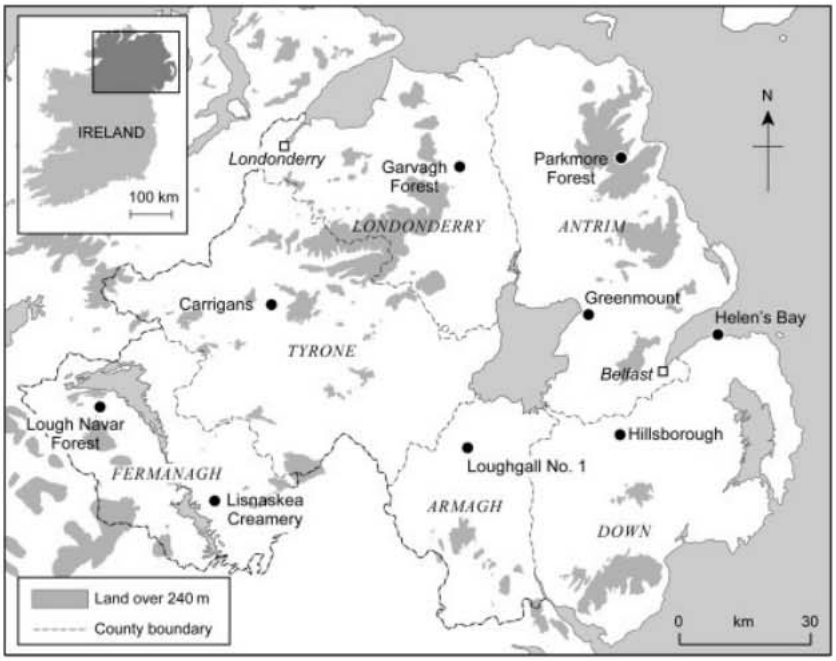

Figure 2. Location of the nine climatological stations employed in the analysis.

Table I. Details of the GCMs used in this study.

GCM	Organisation	Country	Atmospheric resolution (Latitude Longitude)	Key reference
HadCM3	UK Met Office Hadley Centre	UK	2:5 3:75	Gordon *et al.* (2000)
CGCM2	Canadian Centre for Climate Modelling and Analysis	Canada	3:7 3:7	Flato *et al.* (2000)
CSIROMk2	Australian Commonwealth Scientific and Research Organisation	Australia	5:6 3:2	Gordon and O'Farrell (1997)

(HadCM3). The coordinates of the other GCMs are provided in Table I. Extracted predictor variables included mean sea level pressure, geopotential heights, humidity variables, mean temperature, and a range of secondary airflow variables, all for three atmospheric pressure levels.

3.2. Methodology

3.2.1. Predictor screening

All 29 predictor variables were examined on a seasonal basis to test their correlation with each of the two predictands (maximum and minimum temperatures) separately. For each individual season, site, and predictand, the original 29 predictor variables were shortlisted to 12, on the basis of the 12 predictors exhibiting the strongest correlation with the predictand (12 was chosen because this is the maximum number of variables SDSM permits in the subsequent partial correlation analysis). The top 5 predictors from this pool of 12 were then selected on the basis of their unique explanatory power, as determined by the partial correlations statistic. The justification for a cut-off threshold at five predictors was that beyond this number, inclusion of further variables increased model noise and countered the statistical downscaling ethos of selecting a parsimonious data set that included only the most statistically meaningful controls on temperature (e.g. Huth, 2005; Crawford *et al.*, 2007). For each of the two predictands, this produced an optimum predictor set for each site and season. This procedure was conducted using predictor variables from both the IR and NIR grid box, in order to examine differences in the optimum predictor sets depending on which grid box was selected. In deciding which grid box to use for downscaling temperature, comparison of site-specific values of explained variance relating to the optimum predictor sets for the IR and NIR grid boxes were examined. These reveal seasonal and spatial variation in strength of explanation utilising each grid set, with the result that the optimum predictor set from the grid box generally producing higher levels of explained variance would be selected for subsequent downscaling.

3.2.2. Model calibration

When the most appropriate grid box was determined, selected surface and atmospheric predictors were then used to calibrate the statistical transfer functions on a seasonal basis, linking the large-scale variables to the two climate variables of interest, for each site and season. In the same manner as Fealy and Sweeney (2008), predictors that demonstrated a degree of consistency between sites were preferentially selected. This ensured any comparison of results across Northern Ireland could be based on the same set of future controls on temperature. Tables II and III display the most commonly occurring predictors for each season, for maximum and minimum temperatures, respectively. On the basis of the calibrated monthly models (calibrated on the period of 1961–1975), a weather generator within SDSM was then used to generate maximum and minimum temperatures data for each site for the period of 1976–1990. The weather generator produces ensembles of synthetic daily weather series, which helps address uncertainty associated with individual ensemble members (Wilby *et al.*, 2004). Comparison of this generated weather data with the observed data during this time period enabled validation of the model. In addition, the three stations with data spanning 1961–2000 were used to assess the effects of alternative and longer calibration periods. The three stations were: (1) Calibrated on the period of 1961–1990 and validated on the period of 1991–2000; and (2) Calibrated on the period of 1971–2000 and validated on the period of 1961–1970. These periods offered the examination of longer calibration periods on downscaled scenarios, but also crucially the impact of calibration based on warmer periods in the observed record (particularly the 1971–2000 calibration period).

3.2.3. Generating future scenarios

In order to produce site-specific future temperature scenarios, data from the HadCM3, CSIROMk2, and CGCM2 GCMs (both A2 and B2 emissions scenarios) were employed as predictor variables in conjunction with the calibrated transfer functions. This enabled the creation of downscaled future temperature scenarios for the period of 1961–2099 under multiple GCMs and emissions scenarios. Downscaled future maximum and minimum temperatures scenarios for each site, season, GCM and emission scenario were then examined for three thirty-year future time slices centred on the 2020s (2011–2040), 2050s (2041–2070) and 2080s (2070–2099). Results were mapped according to magnitude of warming from the 1961–1990 modelled baseline period. In addition, three of the Statistical and regional dynamical downscaling of extremes for European regions (STARDEX) diagnostic tests (Goodess *et al.*, 2003) for temperature were

Table II. The most consistently highly correlated optimum predictors among all sites for each season for maximum and minimum temperatures using predictors from the NIR grid box. The number represents the number of sites (out of a maximum of nine) at which the named predictor is in the top five for explanatory power.

Winter			Spring		
Predictor	Max temp	Min temp	Predictor	Max temp	Min temp
temp	9	7	temp	9	9
shum	9	7	s850	7	8
s850	9	6	s500	5	8
s500	7	7	p500	4	8
p500	2	9	p8_f	0	7

Summer			Autumn		
Predictor	Max temp	Min temp	Predictor	Max temp	Min temp
temp	7	5	temp	9	8
s850	3	9	p500	8	6
p500	3	8	shum	5	9
shum	3	8	s850	4	9
p5_z	9	0	s500	8	2

Table III. The most consistently highly correlated optimum predictors among all sites for each season for maximum and minimum temperatures using predictors from the IR grid box. The number represents the number of sites (out of a maximum of nine) at which the named predictor is in the top five for explanatory power.

Winter			Spring		
Predictor	Max temp	Min temp	Predictor	Max temp	Min temp
Temp	9	9	temp	9	9
p500	6	8	s850	6	8
p8_f	8	5	p500	1	9
s500	4	9	p8_v	6	2
Shum	7	1	rhum	4	3

Summer			Autumn		
Predictor	Max temp	Min temp	Predictor	Max temp	Min temp
Temp	9	9	temp	9	9
Rhum	3	8	s500	9	6
p5zh	8	2	s850	9	3
s850	3	7	p5zh	8	2
p5_v	8	0	p500	2	8

examined in order to investigate changes in future temperature extremes. An overview of the downscaling process and the key model choices is presented in Table IV.

Table IV. Overview of the downscaling procedure to generate future temperature scenarios for the nine sites employed in this study.

Model issue	Selection
Predictors for maximum temperature	temp, p500, p5_z
Predictors for minimum temperature	temp, p500, shum
Downscaling model structure	Seasonal
Model calibration period	1961–1975
Model validation period	1976–1990
Future downscaled time periods	2011–2040 (2020s); 2041–2070 (2050s); 2070–2099 (2080s)

Key for Tables II–IV

Predictor code	Predictor variable
p500	500 hPa geopotential height
p5_v	500 hPa meridional velocity
p5_z	500 hPa vorticity
p5zh	500 hPa divergence
p850	850 hPa geopotential height
p8_f	850 hPa airflow strength
p8_v	850 hPa meridional velocity
rhum	Near-surface relative humidity
s500	500 hPa specific humidity
s850	850 hPa specific humidity
shum	Near-surface specific humidity
temp	Mean temperature at 2 m

4. Results and discussion

4.1. Predictor selection

The most commonly occurring optimum predictors for maximum and minimum temperatures from both grid boxes are displayed in Tables II and III. Although spatial variation exists with respect to the leading predictor variables, it is much less marked than the spatial variation in the optimum predictor sets noted by Crawford *et al.* (2007) when downscaling precipitation, where a discrete southeast–northwest divide in optimum predictors was apparent. As temperature is a more homogeneous variable than precipitation, this increased spatial uniformity over precipitation is perhaps unsurprising. More notable, however, are the contrasts in optimum predictor sets dependent on season and on which grid box is employed in the analysis. When accounting for temporal changes in optimum predictors, it is helpful to draw on one of the aforementioned criteria of Wilby *et al.* (2002), which state that predictors should be physically and conceptually sensible with respect to the predictand. Providing

wider climatological context is crucial here in linking predictors that demonstrate physically meaningful relationships with maximum and minimum temperatures with those that also exhibit statistical correlations with these predictands. Predictor output from each grid box generally illustrates climatologically meaningful relationships with both temperature variables. Both grid boxes reveal that mean temperature at 2 m is the key predictor variable for both maximum and minimum temperatures across virtually all sites and seasons. Since mean temperature is derived from the average of maximum and minimum temperatures, it is unsurprising that this correlates strongly with both observed maximum and minimum temperatures. In addition, and in the same mould as Widmann *et al*. (2003) when precipitation was used as a predictor for downscaling precipitation, large-scale NCEP mean temperature may integrate many relevant large-scale predictors that explain much of the variance in maximum and minimum temperatures. Other dominant predictors from both grid boxes include moisture variables such as specific humidity at all three atmospheric levels. The direct positive correlation between specific humidity and temperature is responsible for the explanatory power specific humidity exerts on both maximum and minimum temperatures (Barry and Chorley, 1998; Aguado and Burt, 2004). Many aspects of the seasonal variation in the other optimum predictors from each grid box tend to reflect the temporal sequencing of large-scale mid-latitude circulation, with attainment of maximum zonal index and resultant control of westerly airflows across the north of Ireland in autumn and winter, and subsequent westward retreat of these influences in the spring and summer months. The presence of airflow strength predictors in winter (IR grid box) and spring (NIR grid box) reflects the prevalence of a zonal circulation regime and frequency of storms at these periods (Betts, 1997), with this discrepancy in timing perhaps reflecting the extension of depressions with a more northerly trajectory in the spring months, and thus captured only in NIR grid-box output. In addition, zonal flow is a strong predictor for a selection of sites in winter, reflecting the prevalence of westerlies, whilst upper air divergence in autumn facilitates the formation and deepening of depressions at the surface (O'Hare and Sweeney, 1986). Inherent shortening of the upper airflow pattern and subsequent retreat of maritime westerly influences as the continental anticyclone extends towards Ireland in the spring and summer months is reflected by the presence of meridional velocity and geopotential heights as important predictors during these seasons. However, the west–east penetration of depressions is still captured by predictors such as upper air divergence in the summer months in IR grid-box output, reflecting the maritime westerly location of this grid box and its resultant susceptibility to zonal influences throughout the year. The absence of such predictors in NIR grid-box output in summer perhaps reflects the more easterly position of the SB component, decreasing the susceptibility of the NIR grid box to westerly influences in summer. Vorticity is prevalent in both grid boxes during summer, with increased prominence from NIR grid-box output, perhaps again reflecting the influence of the SB component, where localized convection at this time can enhance thunderstorm activity moving inland from the Solway coast in Scotland (Harrison, 1997).

Overall, predictor output from the IR and NIR grid boxes indicate generally similar variables with high explanatory power with respect to maximum and minimum temperatures, with small differences accounted for by geographical factors with respect to each grid box. Predictors largely reflect the seasonal pattern of mid-latitude circulation and thus capture physically meaningful relationships with temperature.

4.2. Grid-box selection

As noted by Brinkmann (2002), predictors from the grid box overlying the target station do not always exhibit the strongest relationships with surface predictands from that station. In this study, the IR grid box directly overlies the island of Ireland, whilst the notional NIR grid box emphasizes the northeasterly location of Northern Ireland within the island of Ireland by averaging output from the IR box with the more northeasterly located SB grid box. Potential spatial offsets in predictor–predictand relationships can thus be examined by analysing output from the NIR grid box. Tables V and VI illustrate that higher levels of explained variance in both maximum and minimum temperatures are achieved when optimum predictors from the NIR grid box are employed as opposed to those from the IR grid box for all sites and seasons. In this respect, the NIR grid box seems more statistically appropriate for downscaling temperature in Northern Ireland. This contrasts with the study of Crawford *et al*. (2007), where the IR grid box emerged as most appropriate for downscaling precipitation over Northern Ireland. However, in the present study, it is important to note that predictors from both grid boxes captured generally high levels of explained variance across all sites and seasons.

These results reveal that the IR and NIR grid boxes are both statistically well correlated with surface temperature, with the NIR grid box emerging as marginally more

Table V. Percentage of explained variance in daily maximum temperature when seasonal models are calibrated using the optimum predictor sets from the IR grid box and the NIR grid box for each site and season.

Max temp stations	Winter		Spring		Summer		Autumn	
	IR	NIR	IR	NIR	IR	NIR	IR	NIR
Greenmount	51	60	65	70	54	58	79	81
Parkmore Forest	51	59	64	68	54	58	78	82
Loughgall	56	63	64	69	51	60	79	81
Garvagh Forest	52	61	63	67	50	54	79	81
Helen's Bay	54	63	61	69	43	47	80	82
Hillsborough	58	66	64	69	50	54	81	83
Lisnaskea Creamery	54	62	63	68	49	60	80	81
Lough Navar Forest	57	64	65	68	50	52	79	81
Carrigans	61	71	79	83	62	64	77	82

Table VI. Percentage of explained variance in daily minimum temperature when seasonal models are calibrated using the optimum predictor sets from the IR grid box and the NIR grid box for each site and season.

Min temp stations	Winter		Spring		Summer		Autumn	
	IR	NIR	IR	NIR	IR	NIR	IR	NIR
Greenmount	57	76	46	59	69	72	49	62
Parkmore Forest	59	74	42	56	66	73	41	67
Loughgall	54	73	49	57	65	72	55	62
Garvagh Forest	55	73	49	58	63	72	47	57
Helen's Bay	61	82	53	63	73	82	62	74
Hillsborough	65	82	59	67	76	81	60	73
Lisnaskea Creamery	57	73	46	58	67	69	46	57
Lough Navar Forest	58	73	52	58	71	74	52	61
Carrigans	63	79	56	67	71	78	56	69

strongly correlated throughout the year at every site. The result that both grid boxes are strongly correlated with temperature corroborates the findings from the optimum predictor tables which suggested that both grid boxes highlighted physically meaningful controls on temperature. In addition, the fact that the NIR grid box, which can be considered the remote grid box in this study, was marginally more strongly correlated illustrates the importance of examining potential spatial offsets in predictor–predictand relationships.

4.3. Impact of the calibration period

Results of the calibration and validation period for maximum and minimum temperatures for all nine stations are displayed in Tables VII and VIII. Pearson's r values in the range of 0.66–0.91 during the calibration period indicate that a significant portion of the variance is captured by the seasonal regression models, which infers a satisfactory modelling of the temperature series in all seasons, particularly during autumn and spring. Summer calibration values tend to be lowest, but still generally reach r values of ca. 0.70–0.75. High Pearson's r values for the validation period illustrate that the modelled temperature series, based upon the calibrated seasonal models, closely mirrors observed data. This indicates that the seasonal forcing component of the large-scale predictors has been adequately captured, offering increased confidence in future projections. Since the original calibration period (1961–1975) represents a period when the dominant mode of atmospheric variability in the North Atlantic, the North Atlantic Oscillation (NAO) (Hurrell, 1995), was in a largely negative phase, and the validation period (1976–1990) was in a largely positive phase, the ability of the transfer functions to reproduce a significant portion of the observed variability over the validation period suggests this particular mode of variability has been adequately captured. In order to capture low-frequency oscillations such as the Atlantic Multidecadal Oscillation (AMO) (Kerr, 2000), however, a 15-year calibration period would be considered insufficient.

Table VII. Pearson's r values for the seasonal calibration (1961–1975) and validation (1976–1990) periods for maximum temperature.

Max temp stations	Winter		Spring		Summer		Autumn	
	Cal.	Val.	Cal.	Val.	Cal.	Val.	Cal.	Val.
Greenmount	0.75	0.74	0.84	0.85	0.74	0.75	0.90	0.88
Parkmore Forest	0.75	0.77	0.82	0.85	0.74	0.77	0.90	0.88
Loughgall	0.77	0.74	0.83	0.85	0.72	0.78	0.90	0.89
Garvagh Forest	0.76	0.75	0.82	0.83	0.70	0.74	0.90	0.89
Helen's Bay	0.77	0.75	0.82	0.84	0.67	0.72	0.90	0.89
Hillsborough	0.80	0.78	0.83	0.85	0.73	0.78	0.91	0.89
Lisnaskea Creamery	0.76	0.74	0.82	0.84	0.72	0.77	0.90	0.89
Lough Navar Forest	0.78	0.77	0.82	0.83	0.69	0.75	0.90	0.89
Carrigans	0.83	0.82	0.91	0.89	0.79	0.83	0.89	0.88

Table VIII. Pearson's r values for the seasonal calibration (1961–1975) and validation (1976–1990) periods for minimum temperature.

Min temp stations	Winter		Spring		Summer		Autumn	
	Cal.	Val.	Cal.	Val.	Cal.	Val.	Cal.	Val.
Greenmount	0.69	0.68	0.81	0.76	0.66	0.68	0.81	0.81
Parkmore Forest	0.69	0.66	0.81	0.76	0.72	0.69	0.83	0.80
Loughgall	0.68	0.66	0.78	0.71	0.67	0.66	0.79	0.81
Garvagh Forest	0.69	0.69	0.77	0.72	0.65	0.66	0.80	0.82
Helen's Bay	0.70	0.72	0.83	0.81	0.74	0.76	0.86	0.84
Hillsborough	0.75	0.75	0.85	0.79	0.74	0.76	0.86	0.85
Lisnaskea Creamery	0.68	0.69	0.76	0.72	0.66	0.65	0.81	0.80
Lough Navar Forest	0.71	0.69	0.78	0.71	0.68	0.63	0.81	0.79
Carrigans	0.75	0.77	0.83	0.79	0.74	0.74	0.84	0.83

Results for the modified calibration and validation periods for the three stations with additional data are displayed in Tables IX and X. Pearson's r values for all three calibration periods do not differ considerably, but some seasonal differences are apparent. A higher proportion of explained variance in maximum temperature is captured by seasonal models calibrated on the longer calibration periods, particularly for spring and summer. For minimum temperature, however, the reverse is generally true, with calibration period 1 achieving highest Pearson's r values throughout the year. Pearson's r values for validation, based upon the three different calibration periods, again show only moderate differences for both maximum and minimum temperatures. Future projections based upon the modified calibration periods (Figure 3) result in only modest differences in future temperature,

Table IX. Pearson's r values for the original and modified seasonal calibration periods for maximum temperature. The highest r value for each site and season for model calibration and validation is highlighted in grey. Calibration period 1: 1961–1975; Calibration period 2: 1961–1990; Calibration period 3: 1971–2000.

	Helen's Bay		Hillsborough		Lough Navar Forest	
	Cal.	Val.	Cal.	Val.	Cal.	Val.
Calibration period			Winter			
1	0.77	0.75	0.80	0.78	0.78	0.77
2	0.77	0.69	0.79	0.71	0.78	0.71
3	0.74	0.76	0.76	0.79	0.75	0.78
Calibration period			**Spring**			
1	0.82	0.84	0.83	0.85	0.82	0.83
2	0.83	0.79	0.84	0.83	0.83	0.82
3	0.83	0.81	0.84	0.82	0.83	0.82
Calibration period			**Summer**			
1	0.67	0.72	0.73	0.78	0.69	0.75
2	0.71	0.71	0.76	0.75	0.74	0.72
3	0.72	0.58	0.78	0.67	0.75	0.61
Calibration period			**Autumn**			
1	0.90	0.89	0.91	0.89	0.90	0.89
2	0.90	0.88	0.90	0.89	0.89	0.88
3	0.90	0.90	0.91	0.91	0.90	0.90

Table X. Pearson's r values for the original and modified seasonal calibration periods for minimum temperature. The highest r value for each site and season for model calibration and validation is highlighted in grey. Calibration period 1: 1961–1975; Calibration period 2: 1961–1990; Calibration period 3: 1971–2000.

	Helen's Bay		Hillsborough		Lough Navar Forest	
	Cal.	Val.	Cal.	Val.	Cal.	Val.
Calibration period			**Winter**			
1	0.70	0.72	0.75	0.75	0.71	0.69
2	0.71	0.63	0.75	0.69	0.71	0.64
3	0.70	0.67	0.74	0.74	0.69	0.71
Calibration period			**Spring**			
1	0.83	0.81	0.85	0.79	0.78	0.71
2	0.82	0.79	0.83	0.80	0.75	0.73
3	0.81	0.84	0.81	0.85	0.73	0.78
Calibration period			**Summer**			
1	0.74	0.76	0.74	0.76	0.68	0.63
2	0.76	0.74	0.76	0.77	0.67	0.64
3	0.77	0.67	0.78	0.68	0.67	0.63
Calibration period			**Autumn**			
1	0.86	0.84	0.86	0.85	0.81	0.79
2	0.86	0.81	0.86	0.84	0.80	0.73
3	0.84	0.84	0.85	0.86	0.77	0.82

with both larger and smaller temperature increases projected at different times of the year.

The findings here indicate that modifying the calibration period can result in small seasonal changes in: (1) The portion of variance captured by the regression models (as expressed by the calibration values); (2) How closely modelled data matches observed data (as expressed by the validation values); and (3) Future

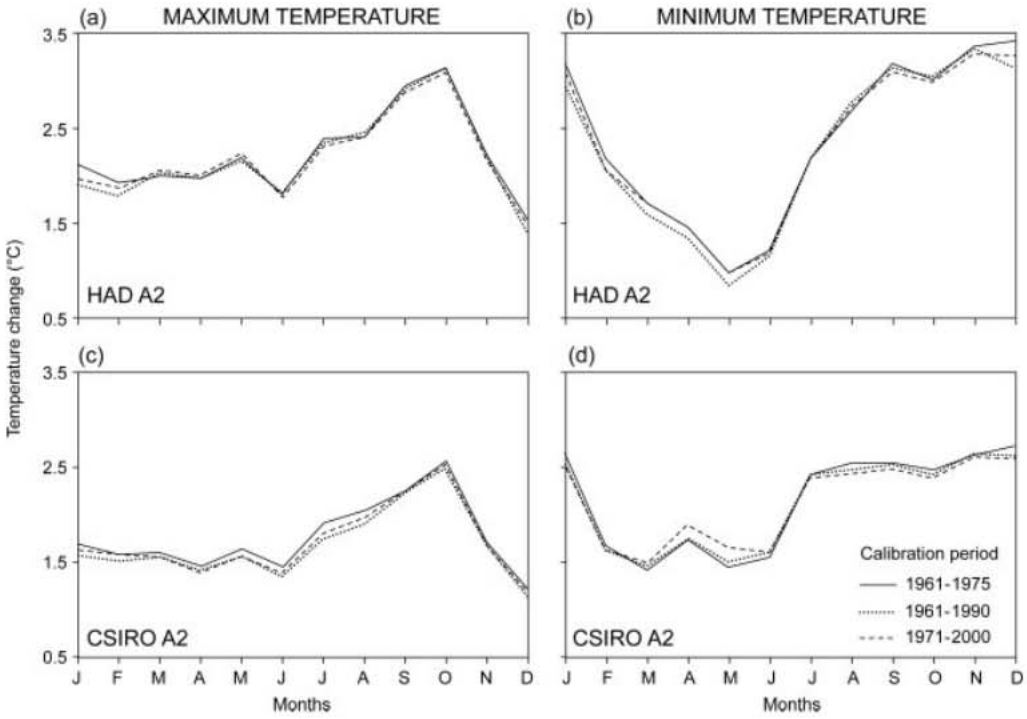

Figure 3. Future scenarios of maximum temperature (left charts) and minimum temperature (right charts) based upon the Had CM3 GCM (upper charts) and the CSIRO MK2 GCM (lower charts) under the A2 emissions scenario for the 2080s when calibrated on period 1 (solid line), period 2 (short dashed line) and period 3 (long dashed line) for Helen's Bay.

temperature changes (as expressed by future downscaled scenarios). The changes in each case are rather minor, and thus increase confidence that calibrating seasonal models on the original period of 1961–1975 is satisfactory for downscaling temperature over Northern Ireland. These results concur with the findings of Anandhi *et al.* (2009), where increasing the calibration period from 6 to 16 years offered no significant improvement when downscaling temperature over India. This indicates that, even where a small time-frame for model calibration exists (15 years in this study), efficient downscaling models can still be constructed. These results also reveal, however, the importance of examining changes in the calibration period in order to deduce whether an extension or modification produces more satisfactory results.

4.4. Mean temperature changes

Table XI displays the change in temperature from the 1961–1990 modelled baseline period for 3 future time slices, when downscaled scenarios are averaged across all 3 GCMs, two emissions scenarios, 4 seasons and 9 sites employed in this study. Results illustrate a progressive warming for all future time slices for both maximum and minimum temperatures, from a 0.8 °C change for the 2020s, up to a 2.2 °C change by the 2080s. Maximum temperature is generally projected to increase marginally more than minimum temperature when averaged on an annual basis. Such results lie within the temperature range indicated in the SNIFFER report and match closely downscaled temperature scenarios for 14 stations across the Republic of Ireland (Fealy and Sweeney, 2008).

4.5. Seasonal temperature changes

Changes in temperature as displayed in Table XI mask important variation among individual scenarios, sites and seasons. Figure 4 illustrates the seasonal variation in maximum and minimum temperatures for the aforementioned three future time periods, as well as displaying the large inter-GCM/emissions scenario differences in temperature changes. For each future time slice, winter and spring minimum temperature is projected to increase slightly more than maximum temperature, with the reverse true of summer and autumn. Autumn is the season projected to experience the most warming, for both maximum and minimum temperatures, with spring projected to increase the least. For example, the projected autumn average increase in maximum temperature across all sites, GCMs and emissions scenarios for the 2080s is 2.6 and just 1.6 °C for spring. These seasonal trends accord closely with those developed by Fealy and Sweeney (2008). In addition to seasonal variation in warming, a larger source of variation exists with temperature projections developed by individual GCMs and emissions scenarios. The inter-GCM/emissions scenario range is high for all seasons for both maximum and minimum temperatures, being at its highest for minimum temperature in winter, where individual scenarios

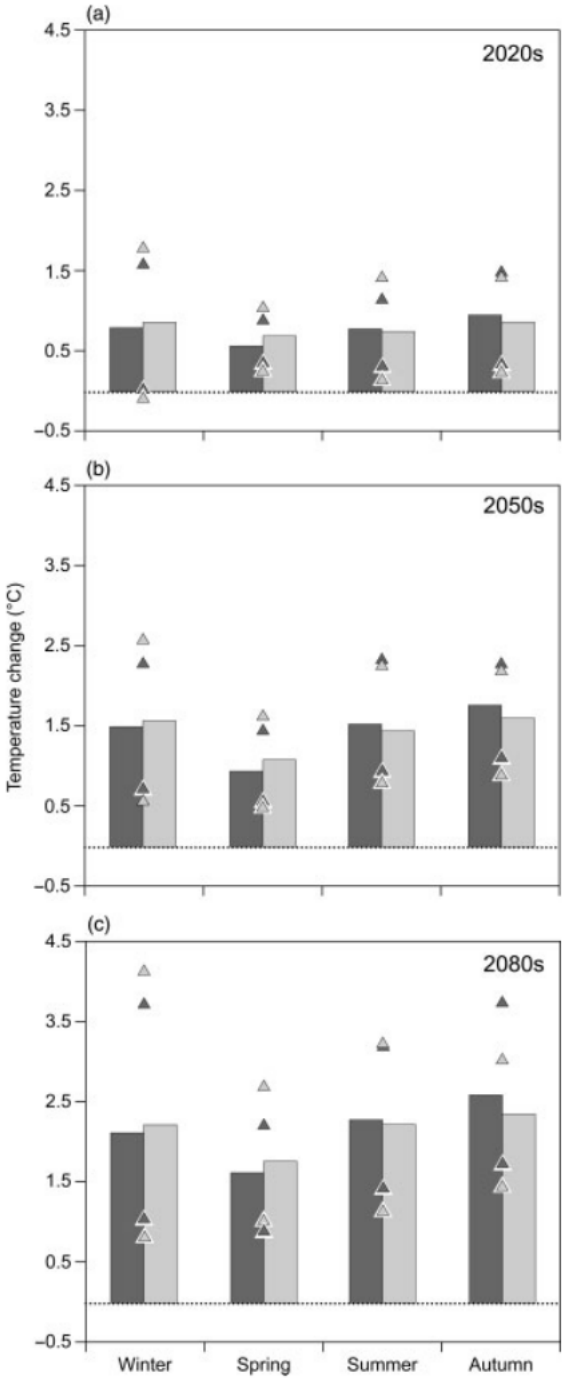

Figure 4. Seasonal changes in maximum temperature (dark bars) and minimum temperature (light bars) for three future time periods. Dark and light triangles represent the full GCM/emissions scenario range for maximum and minimum temperatures, respectively.

Table XI. Average annual temperature change (°C) from the modelled baseline period for three future time slices when averaged across all GCMs, emissions scenarios, sites, and seasons. Also displayed is the full range across all scenarios.

	Max temp	Range	Min temp	Range
2020s	0.8	0.0–1.6	0.8	0.0–1.8
2050s	1.4	0.5–2.3	1.4	0.5–2.6
2080s	2.2	0.9–3.8	2.1	0.8–4.2

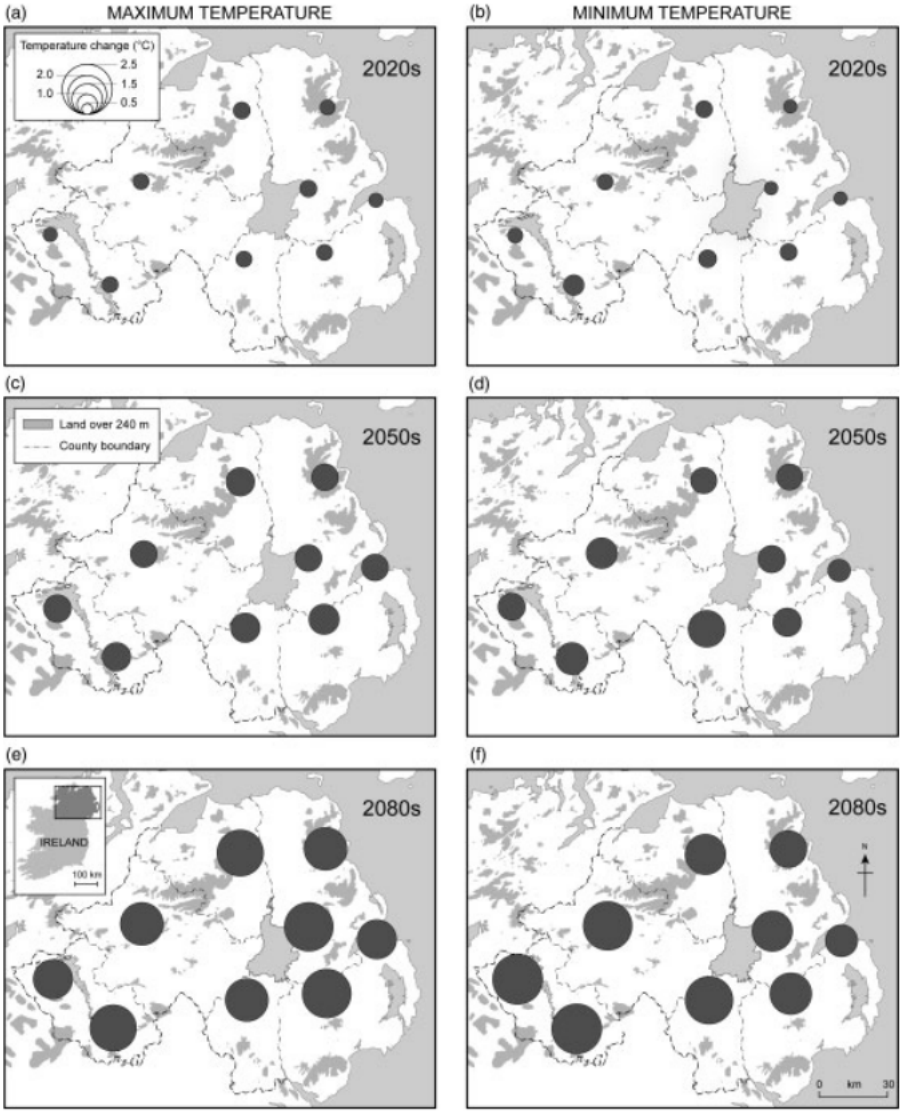

Figure 5. Spatial changes in maximum temperature (left charts) and minimum temperature (right charts) for three future time slices when averaged across all GCMs and emissions scenarios.

range between a 0.8 and a 4.2 °C temperature increase for the 2080s. Such variation illustrates the importance of employing multiple GCMs and emissions scenarios to address uncertainties in individual scenarios.

4.6. Spatial temperature changes

Spatial changes in average annual maximum and minimum temperatures for the 2020s, 2050s, and 2080s is displayed in Figure 5. The spatial pattern emerging from these results is that the magnitude of warming at inland locations is greater than coastal warming for both maximum and minimum temperatures. This pattern becomes more apparent as the decades progress, with annual average differences increasing between inland and coastal locations. For example, in the 2080s, the annual average change in minimum temperature for Helen's Bay (coastal) is 1.7 °C, compared to a 2.4 °C rise for Lisnaskea Creamery (inland). This 'continental' effect is also projected by Fealy and Sweeney (2008).

4.7. Changes in extremes

Given the potential of extreme changes in temperature to have a greater impact on society than the mean climate, it is important to consider changes in some of these extremes with respect to the future temperature scenarios developed in this study. The extremes analysed are defined by thresholds rather than fixed values, with the exception of frost days. The three indices are the hot-day threshold (90th percentile of maximum temperature), the cold-night threshold (10th percentile of minimum temperature) and frost days (number of days below 0 °C) (STARDEX, 2006). As displayed in Table XII, when averaged across all GCMs, emissions scenarios and sites, the hot-day threshold for maximum temperature is projected to increase at a rate in excess of the change in the mean for maximum temperature for the 2020s and 2050s, with the opposite true of the increase in the cold-night threshold for minimum temperature. However, the inter-GCM/emissions scenario range reveals a much wider variation between scenarios for minimum temperature,

Table XII. Changes in three selected temperature extremes for three future time slices. The hot-day threshold and cold-night threshold are changes in °C from the modelled baseline period, whilst no. of frost days is a change in the number of days < 0 °C from the modelled baseline period. The range for each extreme is the full range across GCMs, emissions scenarios and sites.

	Hot-day threshold	Range	Cold-night threshold	Range	No. of frost days	Range
2020s	0.8	0.0–1.7	0.8	0.1–2.7	97	437 to C9
2050s	1.4	0.0–2.4	1.3	0.2–3.2	159	593–0
2080s	2.2	0.3–4.0	2.0	0.8–5.4	219	902–0

where the 2080s range lies between 0.8 and 5.4 °C. For maximum temperature, this range is slightly lower than the range for the mean of maximum temperature. In addition, the number of frost days is projected to decline considerably for all sites, with an average of 219 less frost days over the 30-year period centred on the 2080s from the modelled baseline period.

5. Conclusions

The highest-resolution temperature projections for Northern Ireland, developed from UKCIP02 scenarios for the SNIFFER climate change scoping report (Arkell *et al.*, 2007), were projected across grid cells with a spatial resolution of 50 km. Projections at a finer spatial resolution, however, are increasingly needed as input to impact models. This study has addressed this research need, and developed site-specific future temperature scenarios for nine climatological stations across the north of Ireland. In addition, few studies have explored some of the key issues in the statistical downscaling process, despite their importance in shaping the nature of the future projections. Issues of grid-box choice, the selection of appropriate predictor variables, and the effects of modifying the calibration period were all examined in this study, in an effort to rigorously assess factors with the potential to significantly impact future scenarios.

Results from the grid-box analysis reveal that predictors from both grid boxes highlight physically meaningful predictors and exhibit strong statistical correlations with maximum and minimum temperatures. Ultimately, however, since the more remote NIR grid box is more strongly correlated with each predictand, it appears more appropriate for downscaling temperature in Northern Ireland, thus underlining the importance of examining spatial offsets in predictor–predictand relationships. Whilst it is likely that for much of the year the strongest predictor–predictand relationships exist for the two grid boxes analysed in this study, it is also acknowledged that the examination of additional neighbouring grid boxes could also yield strong correlations at certain time of the year, and thus future studies may benefit from such an investigation. Modifications to the calibration period reveal only marginal increases or decreases in the levels of explained variance captured by the seasonal regression models as well as the resultant effect on the future scenarios. Such minor differences reveal that, where data availability for model calibration is restricted, calibration may still be carried out on the available time-frame with satisfactory results that help place confidence in future projections. It should be noted, however, that longer time periods for calibration may be required to capture low-frequency modes of climate variability. In this respect, we recommend examining the effects of modified and extended calibration periods, if additional data exists for a select number of the sites, in deducing whether the additional data considerably impacts levels of explained variance, and resultant future scenarios.

Future downscaled results exhibit a considerable degree of future warming, with spatial trends indicating greater inland warming, seasonal trends revealing greatest warming in autumn, and extremes analysis indicating hotter hot-day thresholds and cold-night thresholds, and a decline in the number of frost days. These results reveal the potential for considerable environmental and socioeconomic change, with the variation in magnitude of scenarios from individual GCMs and emissions scenarios illustrating the importance of employing multiple scenarios to help address the various sources of uncertainty associated with climate modelling.

The development of site-specific future scenarios represents a significant advance from previous studies where temperature scenarios for Northern Ireland were developed at a coarser spatial resolution. In addition, where previous downscaling studies have largely ignored many of the key processes impacting future scenarios, this study has examined closely some of these aspects with respect to their effect on future projections. The overall findings here highlight the potential of statistical downscaling in developing future scenarios at a spatial resolution matching the requirements of impact modellers, provided a rigorous examination of some of the key processes that impact the nature of the future projections is conducted.

References

Aguado E, Burt JE. 2004. *Understanding weather and climate*, 3rd edn. Pearson Education Inc: New Jersey.

Anandhi A, Srinivas VV, Nagesh Kumar D, Nanjundiah RS. 2009. Role of predictors in downscaling surface temperature to river basin in India for IPCC SRES scenarios using support vector machine. *International Journal of Climatology* **29**: 583–603.

Arkell B, Darch G, McEntee P. (eds). 2007. SNIFFER UKCC13: *Preparing for a changing climate in Northern Ireland*. SNIFFER: Edinburgh.

Arnell NW, Hudson DA, Jones RG. 2003. Climate change scenarios from a regional climate model: Estimating change in runoff in southern Africa. *Journal of Geophysical Research* **108**: 1–17.

Ballester F, Michelozzi P, Iñiguez C. 2003. Weather, climate, and public health. *Journal of Epidemiology and Community Health* **57**: 759–760.

Barry RG, Chorley RJ. 1998. *Atmosphere, Weather and Climate*, 7th edn. Routledge: London and New York.

Bergström S, Carlsson B, Gardelin M, Lindstrom G, Pettersson A, Rummukainen M. 2001. Climate change impacts on runoff in Sweden – assessments by global climate models, dynamical downscaling and hydrological modelling. *Climate Research* **16**: 101–112.

Betts NL. 1997. Climate. In *Soil and environment: Northern Ireland*, Cruickshank JG (ed). Department of Agriculture for Northern Ireland and Queen's University Belfast: Belfast, 63–84.

Betts NL. 2002. Climate Change in Northern Ireland. In *Implications of climate change for Northern Ireland: informing strategy development*, Smyth A, Montgomery WI, Favis-Mortlock DT, Allen S (eds). The Stationery Office Limited: Norwich, 26–42.

Brinkmann WAR. 2002. Local versus remote grid points in climate downscaling. *Climate Research* **21**: 27–42.

Carroll E, Sparks T, Donnelly A, Cooney T. 2009. Irish phenological observations from the early 20th century reveal a strong response to temperature. *Biology & Environment: Proceedings of the Royal Irish Academy* **109**(2): 115–122.

Chapman L, Thornes JE, Huang Y, Sanderson VL, Cai X, White SP. 2008. Modelling of rail temperatures. *Theoretical and Applied Meteorology* **92**: 121–131.

Charles SP, Bates BC, Whetton PH, Hughes JP. 1999. Validation of downscaling models for changed climate conditions: case study of southwestern Australia. *Climate Research* **12**: 1–14.

Crawford T. 2007. *Future Climate Change: Modelling the implications of shifts in rainfall characteristics for runoff in Northern Ireland*. Unpublished Ph.D. thesis, Queen's University Belfast.

Crawford T, Betts NL, Favis-Mortlock D. 2007. GCM grid-box choice and predictor selection associated with statistical downscaling of daily precipitation over Northern Ireland. *Climate Research* **34**: 145–160.

Favis-Mortlock DT, Boardman J. 1995. Nonlinear responses of soil erosion to climate change: a modelling study on the UK South Downs. *Catena* **25**: 365–387.

Fealy R, Sweeney J. 2008. Statistical downscaling of temperature, radiation and potential evapotranspiration to produce a multiple GCM ensemble mean for a selection of sites in Ireland. *Irish Geography* **41**(1): 1–27.

Flato GM, Boer GJ, Lee WG, McFarlane NA, Ramsden D, Reader MC, Weaver AJ. 2000. The Canadian Centre for Climate Modelling and Analysis Global Coupled Model and its Climate. *Climate Dynamics* **166**: 451–467.

Gómez-Heras M, Smith BJ, Fort R. 2006. Surface temperature differences between minerals in crystalline rocks: implications for granular disaggregation of granites through thermal fatigue. *Geomorphology* **78**: 236–249.

Gómez-Martín MB. 2005. Weather, climate and tourism: a geographical perspective. *Annals of tourism research* **32**(3): 571–591.

Goodess CM, Hanson C, Hulme M, Osborn TJ. 2003. Representing climate and extreme weather events in integrated assessment models: a review of existing methods and options for development. *Integrated Assessment* **4**: 145–171.

Gordon C, Cooper C, Senior A, Banks H, Gregory JM, Johns TC, Mitchell JFB, Wood RA. 2000. The simulation of SST, sea ice extents and ocean heat transports in a version of the Hadley Centre coupled model without flux adjustments. *Climate Dynamics* **16**: 147–168. DOI: 10.1007/s003820050010.

Gordon HB, O'Farrell SP. 1997. Transient climate change in the CSIRO coupled model with dynamic sea ice. *Monthly Weather Review* **125**: 875–907.

Handa H, Chapman L, Yao X. 2006. Robust route optimisation for gritting/salting trucks: A CERCIA experience. *Computational Intelligence Magazine* **1**(1): 6–9.

Harrison SJ. 1997. Central and Southern Scotland. In *Regional climates of the British Isles*, Wheeler D, Mayes J (eds). Routledge: London.

Hulme M, Jenkins GJ, Lu X, Turnpenny JR, Michell TD, Jones RG, Lowe J, Murphy JM, Hassell D, Boorman P, MacDonald R, Hill S. 2002. *Climate Change Scenarios for the United Kingdom: The UKCIP02 Scientific Report*. Tyndall Centre for Climate Change Research, School of Environmental Sciences, University of East Anglia: Norwich.

Hurrell JW. 1995. Decadal Trends in the North Atlantic Oscillation: Regional Temperatures and Precipitation. *Science* **269**(5224): 676–679.

Huth R. 2005. Downscaling of humidity variables: a search for suitable predictors and predictands. *International Journal of Climatology* **25**: 243–250.

Kalnay E, Kanamitsu M, Kistler R, Collins W, Deaven D, Gandin L, Iredell M, Saha S, White G, Woollen J, Zhu Y, Leetmaa A, Reynolds B, Chelliah M, Ebisuzaki W, Higgins W, Janowiak J, Mo KC, Ropelewski C, Wang J, Jenne R, Joseph D. 1996. The NCEP/NCAR 40-year reanalysis project. *Bulletin of the American Meteorological Society* **77**: 437–471.

Kerr RA. 2000. A North Atlantic Climate Pacemaker for the Centuries. *Science* **288**(5473): 1984–1985.

Lam JC, Tsang CL, Li DHW. 2004. Long term ambient temperature analysis and energy use implications in Hong Kong. *Energy Conversion and Management* **45**(3): 315–327.

Maraun D, Wetterhall F, Ireson AM, Chandler RE, Kendon EJ, Widmann M, Brienen S, Rust HW, Sauter T, Themeßl M, Venema VKC, Chun KP, Goodess CM, Jones RG, Onof C, Vrac M, Thiele-Eich I. 2010. Precipitation downscaling under climate change. Recent developments to bridge the gap between dynamical models and the end user. *Reviews of Geophysics* **48**, RG3003, 34PP., DOI:10.1029/2009RG000314.

Murphy J. 1999. An evaluation of statistical and dynamical techniques for downscaling local climate. *Journal of Climate* **12**(8): 2256–2284.

Murphy J. 2000. Predictions of Climate Change over Europe using Statistical and Dynamical Downscaling techniques. *International Journal of Climatology* **20**: 489–501.

Nakicenovic N, Alcamo J, Davis G, de Vries B, Fenhann J, Gaffin S, Gregory K, Grübler A, Jung TY, Kram T, La Rovere EL, Michaelis L, Mori S, Morita T, Pepper W, Pitcher H, Price L, Riahi K, Roehrl A, Rogner HH, Sankovski A, Schlesinger M, Shukla P, Smith S, Swart R, van Rooijen S, Victor N, Dadi Z. 2000. *IPCC Special Report on Emissions Scenarios*. Cambridge University Press: Cambridge, United Kingdom and New York, NY, USA, 599 pp.

O'Hare G, Sweeney J. 1986. *The Atmospheric System: Conceptual frameworks in Geography*. Oliver and Boyd: London.

Schubert S, Henderson-Sellers A. 1997. A statistical model to downscale local daily temperature extremes from synoptic-scale atmospheric circulation patterns in the Australian region. *Climate Dynamics* **13**: 223–234.

STARDEX. 2006. Downscaling climate extremes. Available from: http://www.cru.uea.ac.uk/projects/stardex/

Thornton PK, van de Steega J, Notenbaerta A, Herreroa M. 2009. The impacts of climate change on livestock and livestock systems in developing countries: A review of what we know and what we need to know. *Agricultural Systems* **101**(3): 113–127.

Von Storch H, Zorita E, Cubasch U. 1993. Downscaling of global climate change estimates to regional scales: An application to Iberian rainfall in wintertime. *Journal of Climate* **6**: 1161–1171.

Widmann M, Bretherton CS, Salathé Jr EP. 2003. Statistical precipitation downscaling over the Northwestern United States using numerically simulated precipitation as a predictor. *Journal of Climate* **16**(5): 799–816.

Wiik L, Ewaldz T. 2009. Impact of temperature and precipitation on yield and plant diseases of winter wheat in southern Sweden 1983–2007. *Crop Protection* **28**(11): 952–962.

Wilby RL. 1997. Non-stationarity in daily precipitation series: implications for GCM down-scaling using atmospheric circulation indices. *International Journal of Climatology* **17**: 439–454.

Wilby RL. 1998. Statistical downscaling of daily precipitation using daily airflow and teleconnection indices. *Climate Research* **10**: 163–178.

Wilby RL, Charles SP, Zorita E, Timbal B, Whetton P, Mearns OL. 2004. *Guidelines for the use of Climate scenarios developed from Statistical downscaling methods*. Available at http://ipcc-ddc.cru.uea.ac.uk/guidelines/dgm_no2_v1_09_2004.pdf

Wilby RL, Dawson CW. 2001. *Using SDSM Version 2.2- A decision support tool for the assessment of regional climate change impacts, Version 2.2 User Manual*. King's College London: London.

Wilby RL, Dawson CW. 2007. *SDSM 4.2- A decision support tool for the assessment of regional climate change impacts, Version 4.2 User Manual*. Lancaster University: Lancaster/Environment Agency of England and Wales.

Wilby RL, Dawson CW, Barrows EM. 2002. SDSM- a decision support tool for the assessment of regional climate change impacts. *Environmental Modelling and Software* **17**: 147–159.

Wilby RL, Harris I. 2006. A framework for assessing uncertainties in climate change impacts: low flow scenarios for the River Thames, UK. *Water Resources Research* **42**(2): W02419.1–W02419.10.

Wilby RL, Wigley TML. 2000. Precipitation predictors for downscaling: Observed and general circulation model relationships. *International Journal of Climatology* **20**: 641–661.

Wilks DS. 2006. *Statistical methods in the Atmospheric Sciences*, 2nd edn. Academic Press/Elsevier.

